GEOPHYSICS, VOL. 71, NO. 3 (MAY-JUNE 2006); P. O1–O8, 6 FIGS.
10.1190/1.2194512

P-Wave seismic attenuation by slow-wave diffusion: Effects of inhomogeneous rock properties

José M. Carcione[1] and Stefano Picotti[1]

ABSTRACT

Recent research has established that the dominant P-wave attenuation mechanism in reservoir rocks at seismic frequencies is because of wave-induced fluid flow (mesoscopic loss). The P-wave induces a fluid-pressure difference at mesoscopic-scale inhomogeneities (larger than the pore size but smaller than the wavelength, typically tens of centimeters) and generates fluid flow and slow (diffusion) Biot waves (continuity of pore pressure is achieved by energy conversion to slow P-waves, which diffuse away from the interfaces). In this context, we consider a periodically stratified medium and investigate the amount of attenuation (and velocity dispersion) caused by different types of heterogeneities in the rock properties, namely, porosity, grain and frame moduli, permeability, and fluid properties. The most effective loss mechanisms result from porosity variations and partial saturation, where one of the fluids is very stiff and the other is very compliant, such as, a highly permeable sandstone at shallow depths, saturated with small amounts of gas (around 10% saturation) and water. Grain- and frame-moduli variations are the next cause of attenuation. The relaxation peak moves towards low frequencies as the (background) permeability decreases and the viscosity and thickness of the layers increase. The analysis indicates in which cases the seismic band is in the relaxed regime, and therefore, when the Gassmann equation can yield a good approximation to the wave velocity.

INTRODUCTION

Recent studies (e.g., Pride et al., 2004) have shown that the major cause of attenuation in porous media is wave-induced fluid flow, which occurs at different spatial scales: macroscopic, mesoscopic, and microscopic. The attenuation mechanism predicted by the Biot theory (Biot, 1962; Carcione, 2001) has a macroscopic nature. It is the wavelength-scale equilibration between the peaks and troughs of the fast P-wave. Geertsma and Smit (1961) showed that the dissipation factor $(1/Q)$ of the fast P-wave can be approximated by that of a Zener model (Ben-Menahem and Singh, 1981) if the quality factor satisfies $Q > 5$. They obtained the expression:

$$Q^{-1}(\omega) = \frac{\omega(\tau_\epsilon - \tau_\sigma)}{1 + \omega^2\tau_\epsilon\tau_\sigma}, \quad \tau_\sigma = \left(\frac{v_G}{v_{\infty+}}\right)^2\tau_\epsilon, \quad \tau_\epsilon = \frac{A\kappa\rho}{\eta}, \tag{1}$$

where ω is the angular frequency, $v_{\infty+}$ is the P-wave velocity at the high-frequency limit, v_G is Gassmann's velocity (e.g., Carcione, 2001), κ is the permeability, η is the fluid viscosity,

$$\rho = (1 - \phi)\rho_s + \phi\rho_f \tag{2}$$

is the bulk density, ϕ is the porosity, ρ_s is the density of the grains, ρ_f is the fluid density, and $A = \rho_f\mathcal{T}/(\rho\phi) - (\rho_f/\rho)^2$, where $\mathcal{T}$ is the tortuosity. Since the location of the Zener relaxation peak is $\omega_B = 1/\sqrt{\tau_\sigma\tau_\epsilon}$ and $f_B = \omega_B/2\pi$, we obtain

$$f_B = \left(\frac{v_{\infty+}}{v_G}\right)\frac{\eta}{2\pi A\kappa\rho} \approx \frac{\eta}{2\pi A\kappa\rho} = \frac{\phi\eta\rho}{2\pi\kappa\rho_f(\rho\mathcal{T} - \phi\rho_f)}. \tag{3}$$

This equation shows that the peak moves towards the high frequencies with increasing viscosity and decreasing permeability. This means that, at low frequencies, attenuation decreases with increasing viscosity (or decreasing permeability). This contradicts experimental data (e.g., Jones, 1986). Another apparent drawback of the Biot theory is that the macroscopic-flow mechanism underestimates the velocity dispersion and attenuation in rocks (e.g., Mochizuki, 1982; Dvorkin et al., 1995; Arntsen and Carcione, 2001).

Manuscript received by the Editor November 29, 2004; revised manuscript received October 24, 2005; published online May 22, 2006.
[1]Istituto Nazionale di Oceanografia e di Geofisica Sperimentale (OGS), Borgo Grotta Gigante 42c, 34010 Sgonico, Trieste, Italy. E-mail: jcarcione@ogs.trieste.it; spicotti@ogs.trieste.it

It is common to invoke non-Biot attenuation mechanisms to explain low-frequency (seismic and sonic) attenuation in rocks. These mechanisms are the so-called *local fluid flow* or *squirt flow absorption mechanisms*,which have been extensively discussed in the literature (O'Connell and Budiansky, 1974; Dvorkin et al., 1995; Mavko et al., 1998). In this mechanism, fluid-filled microcracks respond with greater fluid-pressure changes than the main pore space. The resulting flow at this microscopic level is responsible for the energy loss. These models have the proper dependence on viscosity with the center frequency of the attenuation peak inversely proportional to fluid viscosity. However, it has been shown that this mechanism is incapable of describing the measured levels of dissipation at seismic frequencies (Diallo et al., 2003; Pride et al., 2004).

Pride et al. (2004) have shown that attenuation and velocity-dispersion measurements can be explained by the combined effect of mesoscopic-scale inhomogeneities and energy transfer between wave modes. They refer to this mechanism as mesoscopic loss. The mesoscopic-scale length is intended to be much larger than the grain sizes but much smaller than the wavelength of the pulse. For instance, if the fluid compressibility varies significantly from point to point, diffusion of pore fluid between different regions constitutes a mechanism that can be important at seismic frequencies. White (1975) and White et al. (1975) were the first to introduce the mesoscopic-loss mechanism based on approximations in the framework of Biot theory. They considered gas pockets in a water-saturated porous medium and porous layers alternately saturated with water and gas, respectively. These are the first so-called *patchy saturation* models. Dutta and Odé (1979a, b) and Dutta and Seriff (1979) solved the problem exactly by using Biot theory and confirmed the accuracy of White's results.[2]

The mesoscopic-loss theory has been further refined by Norris (1993), Gurevich and Lopatnikov (1995), Gelinsky and Shapiro (1997), Gurevich et al. (1997), Shapiro and Müller (1999), Johnson (2001), Müller and Gurevich (2004a), and Pride et al. (2004). Gurevich et al. (1997) obtained the P-wave quality factor as a function of frequency for 1D finely layered poroelastic media (normal to layering). They considered Biot's loss, scattering, and mesoscopic-flow loss, and found that the quality factor is approximately given by the harmonic average of the corresponding single quality factors. Shapiro and Müller (1999) reinterpreted the role of the hydraulic permeability in the mesoscopic-flow mechanism, concluding that this permeability corresponds to the zero-frequency limit of the seismic permeability actually controlling the loss. Müller and Gurevich (2004a) performed numerical experiments in random and periodic media with patchy saturation (gas and water) with a correlation length of 20 cm, showing attenuation peaks in the seismic band and at 80% water saturation.

Johnson (2001) developed a generalization of White's model for patches of arbitrary shape. This model has two geometrical parameters, besides the usual parameters of Biot theory: the specific surface area and the size of the patches. Patchy saturation effects on acoustic properties have been observed by Murphy (1982) and Knight and Nolen-Hoeksema (1990). Cadoret et al. (1995) investigated the phenomenon in the laboratory at the frequency range 1–500 kHz. Two different saturation methods result in different fluid distributions and produce two different values of velocity for the same saturation. Imbibition by depressurization produces a very homogeneous saturation, while drainage by drying produces heterogeneous saturations at high water saturation levels. In the latter case, the experiments show considerably higher velocities, as predicted by White's model.

Carcione et al. (2003) performed numerical-modeling experiments based on Biot's equations of poroelasticity and White's model of regularly distributed spherical gas inclusions. They showed that attenuation and velocity dispersion measurements can be explained by the combined effect of mesoscopic-scale inhomogeneities and energy transfer between wave modes. By using computerized tomography (CT) scans, it is possible to visualize the fluid distribution and spatial heterogeneities in real rocks (Cadoret et al., 1995). Fractal models, such as the von Kármán correlation function, calibrated by the CT scans, were used by Helle et al. (2003) to model heterogeneous rock properties and perform numerical experiments based on Biot's equations of poroelasticity.

In this work, we use the model of White et al. (1975) for the investigation. It is mathematically simple and allows us to model different mesoscopic-scale heterogeneities. Dutta and Seriff (1979) have shown that the effects of geometry are not significant, so the qualitative aspects of the physics have a general validity. Another feature in favor of the periodic system is that the dissipation factor $1/Q$ is proportional to ω and $1/\sqrt{\omega}$ at the low- and high-frequency limits, respectively. This is the behavior recently found by Müller and Gurevich (2004b) for 3D porous media with any type of random inhomogeneity. We consider different cases and compare the phase velocities and loss angles to determine the effects of the inhomogeneities.

COMPLEX BULK MODULUS

We consider a periodic layered system composed of porous media 1 and 2 with thickness d_l, $l = 1,2$ and period $d_1 + d_2$. White et al. (1975) obtained the complex modulus for a P-wave traveling along the direction perpendicular to the stratification. It is given by

$$E = \left[\frac{1}{E_0} + \frac{2(r_2 - r_1)^2}{\mathrm{i}\omega(d_1 + d_2)(I_1 + I_2)} \right]^{-1}, \tag{4}$$

where

$$E_0 = \left(\frac{p_1}{E_{G_1}} + \frac{p_2}{E_{G_2}} \right)^{-1}, \tag{5}$$

with $p_l = d_l/(d_1 + d_2)$, $l = 1,2$. Omitting the subindex l for clarity, we have for each medium

$$E_G = K_G + \frac{4}{3}\mu_m, \tag{6}$$

where K_G is the Gassmann modulus and μ_m is the dry-rock (matrix or frame) shear modulus. The Gassmann modulus is given by

[2]Dutta and Seriff (1979) point out a mistake in White (1975), where White uses the P-wave modulus instead of the bulk modulus to derive the complex bulk modulus.

$$K_G = K_m + \alpha^2 M, \tag{7}$$

where

$$\alpha = 1 - \frac{K_m}{K_s}, \tag{8}$$

$$M = \frac{K_s}{1 - \phi - K_m/K_s + \phi K_s/K_f}, \tag{9}$$

K_s is the solid-grain bulk modulus, K_f is the fluid bulk modulus, and K_m is the dry-rock bulk modulus (e.g., Mavko et al., 1998; Carcione, 2001).

Moreover,

$$r = \frac{\alpha M}{E_G} \tag{10}$$

is the ratio of fast P-wave fluid tension to total normal stress,

$$I = \frac{\eta}{\kappa k} \coth\left(\frac{kd}{2}\right) \tag{11}$$

is an impedance related to the slow P-wave,

$$k = \sqrt{\frac{i\omega\eta}{\kappa K_E}} \tag{12}$$

is the complex wavenumber of the slow P-wave, and

$$K_E = \frac{E_m M}{E_G} \tag{13}$$

is an effective modulus, with

$$E_m = K_m + \frac{4}{3}\mu_m, \tag{14}$$

the dry-rock fast P-wave modulus.

Let us assume in the following analysis that the properties of the frame are the same in media 1 and 2 and that the contrast is because of two different saturating fluids (for example, water and gas). The approximate transition frequency separating the relaxed and unrelaxed states (i.e., the approximate location of the relaxation peak) is

$$f_m = \frac{8\kappa_1 K_{E_1}}{\pi\eta_1 d_1^2} \tag{15}$$

(Dutta and Seriff, 1979; Carcione et al., 2003), where the subindex 1 refers to water for a layered medium alternately saturated with water and gas. At this reference frequency, the Biot slow-wave attenuation length equals the mean layer thickness or characteristic length of the inhomogeneities (Gurevich and Lopatnikov, 1995) (see below). Equation 15 indicates that the mesoscopic-loss mechanism moves towards the low frequencies with increasing viscosity and decreasing permeability, i.e., the opposite behavior of the Biot relaxation mechanism, whose peak frequency is given by equation 3.

The mesoscopic mechanism results from the presence of the Biot slow wave, and the diffusivity constant is $\gamma = \kappa K_E/\eta$. The critical fluid-diffusion relaxation length L is obtained by setting $|kL| = 1$, where k is the wavenumber (equation 12). It gives $L = \sqrt{\gamma/\omega}$. The fluid pressures will be equilibrated if L is comparable to the period of the stratification. For smaller diffusion lengths (e.g., higher frequencies), the pressures will not be equilibrated, causing attenuation and velocity dispersion. Notice that the reference frequency (equation 15) is obtained for a diffusion length $L = d_1/4$.

At sufficiently low frequencies, the fluid pressure is uniform (isostress state), and the effective modulus of the pore fluid is given by Wood's law (Wood, 1955):

$$\frac{1}{K_f} = \frac{p_1}{K_{f_1}} + \frac{p_2}{K_{f_2}}. \tag{16}$$

It can be shown (e.g., Johnson, 2001) that $E(\omega = 0)$ is equal to the plane-wave modulus (equation 6) for a fluid whose composite modulus is given by equation 16. On the other hand, at high frequencies, the pressure is not uniform, but can be assumed to be constant within each phase. In such a situation, Hill's theorem (Hill, 1964) gives the high-frequency limit $E(\omega = \infty) = E_0$ (see equation 5).

PHASE VELOCITY AND LOSS ANGLE

The complex bulk modulus (equation 4) can be expressed as $E = |E|\exp(i\theta)$, where θ is the loss angle. We use the concept of complex velocity to obtain the phase velocity and loss angle. If ρ is the bulk density (equation 2), the complex velocity v is defined by the relation $\bar{\rho}v^2 = E$, where $\bar{\rho} = p_1\rho_1 + p_2\rho_2$ is the averaged density. Then, the phase velocity and loss angle are given by

$$v_p = \left[\mathrm{Re}\left(\frac{1}{v}\right)\right]^{-1} \tag{17}$$

and

$$\theta = \tan^{-1}\left[\frac{\mathrm{Im}(v^2)}{\mathrm{Re}(v^2)}\right], \tag{18}$$

where Re and Im denote real and imaginary parts, respectively. The relation between the loss angle and the standard definition of quality factor in viscoelasticity is $Q^{-1} = \tan\theta$.

NUMERICAL EXAMPLES

Fluid properties

The properties of the fluids depend on temperature and pressure, which in turn depend on depth z. A simple (reference) situation is to consider a constant geothermal gradient G, so that the temperature variation with depth is $T = T_0 + Gz$, where T_0 is the surface temperature. A typical value of G is 30°C/km, so that for T_0

= 0°C, T = 30°C at 1 km and T = 105°C at 3.5 km. The absolute pore pressure p at depth z depends on many factors, most of them of geologic nature, such as low-permeability regions, sealing faults, and hydrocarbon caps, which prevent pressure equilibration (communication) from the reservoir to the surface. A reference value is when there are no permeability barriers and the fluid (e.g., water) is free to flow from depth z to the surface. In this case, the pore pressure is hydrostatic and is given by $p = \rho_w g z$, where ρ_w is the water (brine) density and g = 9.81 m/s^2 is the acceleration of gravity. If ρ_w = 1040 kg/m^3, we obtain p = 10 MPa at 1 km and p = 35 MPa at 3.5 km.

We assume that the properties of water do not change significantly with depth. We consider K_w = 2.25 GPa, ρ_w = 1040 kg/m^3, and η_w = 0.003 Pa s (3 cp). In situ reservoir gas behaves as a real gas, which satisfies approximately the van der Waals equation (Friedman, 1963):

$$(p + a\rho_g^2)(1 - b\rho_g) = \rho_g R(T + 273), \tag{19}$$

where T is the temperature in degrees Celsius, p is the gas pressure, ρ_g is the gas density, and R = 8.31 J/(mol°K) = 519.4 J/(kg°K) is the gas constant. For methane (CH_4), a = 0.225 Pa (m^3/mole)^2 = 879.9 Pa (m^3/kg)^2 and b = 42.7 cm^3/mole = 2.675 × 10^{-3}m^3/kg (one mole of methane corresponds to 16 g). The critical pressure and temperature are 4.6 MPa and −82.7°C, respectively. For temperatures above the critical temperature, there is one physically meaningful density for a given pressure. Equation 19 gives the gas density as a function of pressure and temperature, which can be related to depth, if we assume that the gas pressure is equal to the expected formation pressure.

The adiabatic bulk modulus depends on pressure. It can be calculated from the van der Waals equation as $K_g = 4\rho_g\left(\frac{\partial p}{\partial \rho_g}\right)/3$, to obtain

$$K_g = \frac{4}{3}\left[\frac{\rho_g R(T + 273)}{(1 - b\rho_g)^2} - 2a\rho_g^2\right] \tag{20}$$

(Morse and Ingard, 1986). The calculations yield K_g = 0.012 GPa and ρ_g = 78 kg/m^3 at 1-km depth, and K_g = 0.081 GPa and ρ_g = 170 kg/m^3 at 3.5-km depth. The gas viscosity is assumed to be constant and equal to 0.00015 Pa · s.

Frame (matrix) properties

Variable permeability implies changes in porosity and dry-rock moduli. Porosity and permeability are related by the Kozeny-Carman relation

$$\kappa = \frac{B\phi^3 D^2}{(1 - \phi)^2} \tag{21}$$

(Mavko et al., 1998), where D is the grain diameter and B = 0.003.

We use the model of Krief et al. (1990) to obtain the dry-rock moduli K_m and μ_m. The porosity dependence is consistent with the concept of critical porosity, because the moduli should be small above a certain value of the porosity (usually from 0.4 to 0.6). The moduli are given by

$$K_m = K_s(1 - \phi)^{4/(1-\phi)},$$

$$\mu_m = K_m\mu_s/K_s, \tag{22}$$

where K_s and μ_s are the bulk and shear moduli of the solid grains.

We consider six cases divided in subcases.

Case A

Media 1 and 2 have the same properties, and we vary a single specific property of medium 2 by the same percentage (20%), without changing the others or using the relations in equations 2, 21, and 22. We assume $d_1 = d_2$ = 0.2 m. The properties of medium 1 (a water-saturated sandstone) are K_{s_1} = 37 GPa, μ_{s_1} = 44 GPa, ρ_{s_1} = 2650 Kg/m^3 (quartz), ϕ = 0.3, K_{m_1} = 4.8 GPa, μ_{m_1} = 5.7 GPa, κ_1 = 1 Darcy (D_1 = 80 μm), K_{f_1} = 2.25 GPa, ρ_{f_1} = 1040 Kg/m^3, and η_1 = 0.003 Pa · s. Since r (equation 10) does not depend on κ and η, the plane modulus (equation 4) is constant, real, and equal to E_0 for variations of the permeability and viscosity in medium 2. Hence, there is no attenuation in this case.

The subcases are:

- A1—Porosity, ϕ_2 = 0.1
- A2—Frame bulk modulus, K_{m_2} = 1.6 GPa
- A3—Grain properties, K_{s_2} = 12.3 GPa
- A4—Fluid properties, K_{f_2} = 0.75 GPa.

Figure 1 shows the phase velocity (a) and phase angle (and quality factor) (b) corresponding to the different subcases. The vertical

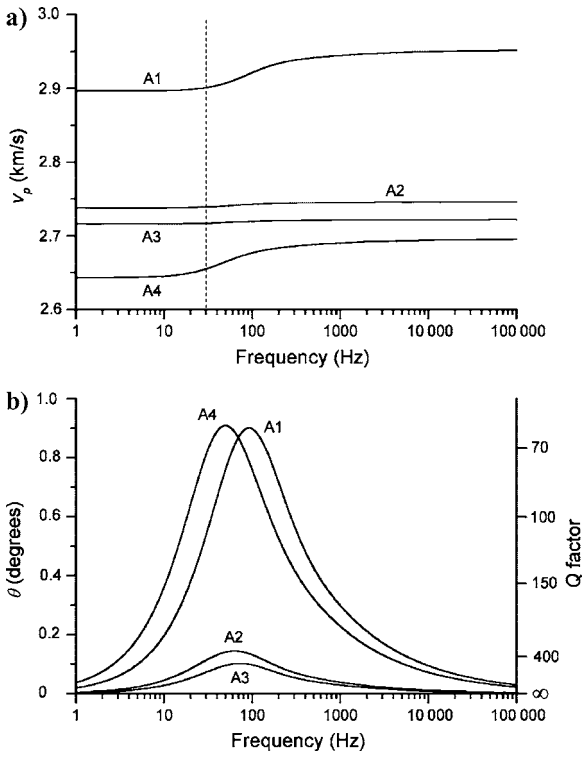

Figure 1. Phase velocity (a) and phase angle (and quality factor) (b), where we vary a single specific property of medium 2 by the same percentage (20%). A1: Porosity; A2: Frame bulk modulus; A3: Grain properties; A4: Fluid properties. The porosity, permeability, and frame modulus are not related by equations 21 and 22, i.e., when one property varies, the others remain constant. The vertical dashed line in (a) indicates a frequency of 30 Hz, i.e., ω = 2 π 30 Hz.

dashed line in (a) corresponds to a frequency of 30 Hz. It indicates the location of the seismic band in terms of the relaxed and unrelaxed states of the rock. In the case of partial saturation, this line gives an estimation of the approximation incurred when using Gassmann modulus (and Wood's mixing law for the fluid phases) or Hill's average (equation 5) to describe the P-wave modulus. The porosity and fluid-modulus contrasts (cases A1 and A4) cause a strong attenuation, with nearly 50 m/s velocity dispersion. Grain- (A3) and frame-moduli (A2) variations are much less significant.

Case B

The two media have the same frame (sandstone, as medium 1 of case A), $d_1 = d_2 = 0.2$ m, medium 1 has water, and medium 2 has gas at 1-km-depth conditions. The subcases are:

- B1—$\kappa_1 = \kappa_2 = 0.1$ D
- B2—$\kappa_1 = \kappa_2 = 1$ D
- B3—$\kappa_1 = \kappa_2 = 10$ D
- B4—$\kappa_1 = 0.1$ D and $\kappa_2 = 10$ D
- B5—$\kappa_1 = 10$ D and $\kappa_2 = 0.1$ D.

Permeability and viscosity describe the mobility of the fluid in the pore space. An increase in permeability (or decrease in viscosity) increases mobility. Figure 2 shows the corresponding phase velocities (a) and loss angles (b) for case B. The relaxation peak moves towards high frequencies for increasing permeability (see curves B1, B2, and B3), in agreement with equation 15, and the maximum loss is the same for the three subcases. Subcases B4 and B5 indicate that it is the permeability of the region hosting the stiffest fluid that determines the location of the relaxation peak (compare to cases B1 and B3, respectively).

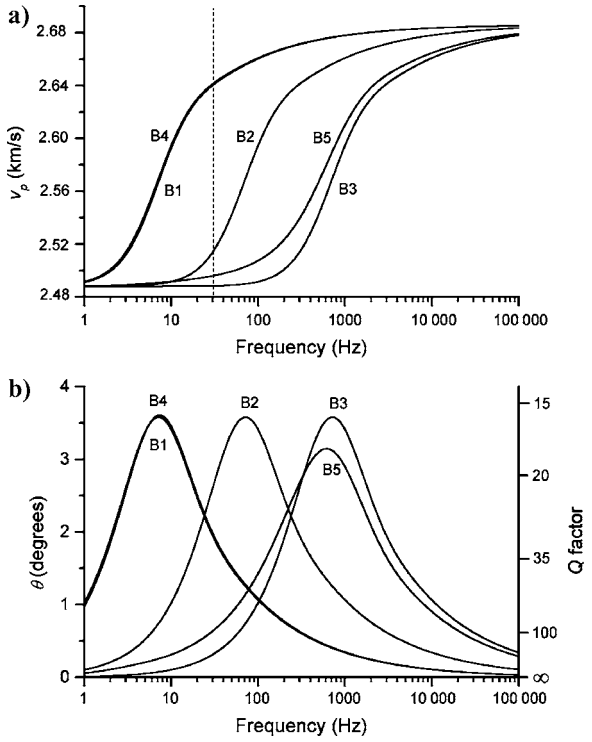

Figure 2. Phase velocity (a) and phase angle (and quality factor) (b) for a sandstone saturated with 50% water and 50% gas. The curves correspond to different permeability values: B1: $\kappa_1 = \kappa_2 = 0.1$ D; B2: $\kappa_1 = \kappa_2 = 1$ D; B3: $\kappa_1 = \kappa_2 = 10$ D; B4: $\kappa_1 = 0.1$ D and $\kappa_2 = 10$ D; B5: $\kappa_1 = 10$ D and $\kappa_2 = 0.1$ D. As in Figure 1, the porosity, permeability, and frame modulus are not related by equations 21 and 22.

Case C

The two media have the same frame (sandstone, as medium 1 of case A), $d_1 = d_2 = 0.2$ m, medium 1 has water, and medium 2 has oil, whose properties are $K_{f_2} = 0.7$ GPa and $\rho_{f_2} = 700$ kg/m^3.

The subcases are

- C1—$\eta_2 = 0.001$ Pa s (1 cp)
- C2—$\eta_2 = 0.01$ Pa s (10 cp)
- C3—$\eta_2 = 0.1$ Pa s (100 cp).

The results, displayed in Figure 3, show that the relaxation peak moves towards low frequencies for increasing viscosity, in agreement with equation 15. Attenuation increases or decreases with viscosity, depending on the value of the frequency, but the maximum loss decreases with increasing viscosity.

Case D

The two media have the same frame (sandstone, as medium 1 of case A), medium 1 has water, and medium 2 has gas at 1-km-depth conditions. The subcases are

- D1—$d_1 = d_2 = 0.1$ m
- D2—$d_1 = d_2 = 0.2$ m
- D3—$d_1 = d_2 = 0.4$ m.

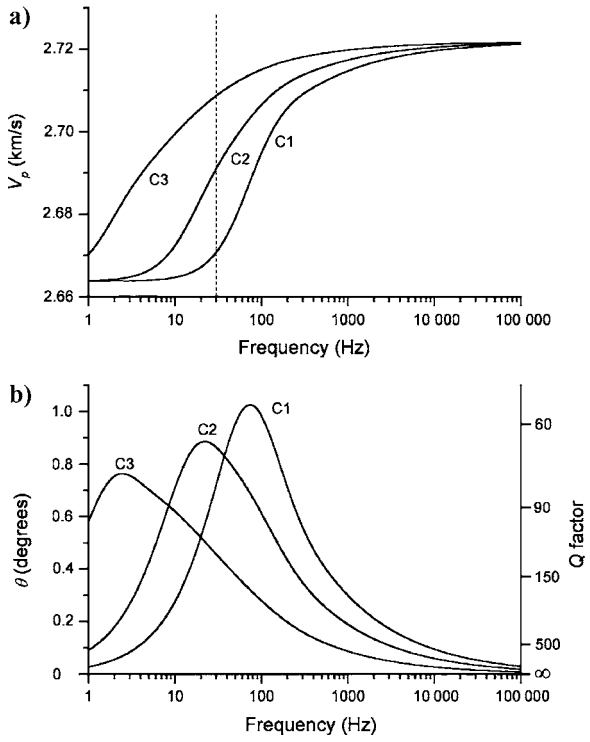

Figure 3. Phase velocity (a) and phase angle (and quality factor) (b) for a sandstone saturated with 50% water and 50% oil. The curves correspond to different oil viscosities: C1: $\eta_2 = 1$ cp; C2: $\eta_2 = 10$ cp; C3: $\eta_2 = 100$ cp.

As predicted by equation 15, when d_1 increases (i.e., the saturation of the stiffest fluid increases), the relaxation peak moves towards low frequencies (see Figure 4). The maximum loss is the same for the three relaxation peaks.

Case E

The two media have the same frame (sandstone, as medium 1 of case A), medium 1 has water, and medium 2 has gas. This case models the patchy-saturation situation. The subcases are

- E1—1-km-depth gas, $d_1 = 0.04$ m ($p_1 = 0.1$) and $d_2 = 0.36$ m ($p_2 = 0.9$)
- E2—1-km-depth gas, $d_1 = 0.2$ m ($p_1 = 0.5$) and $d_2 = 0.2$ m ($p_2 = 0.5$)
- E3—1-km-depth gas, $d_1 = 0.36$ m ($p_1 = 0.9$) and $d_2 = 0.04$ m ($p_2 = 0.1$)
- E4—3.5-km-depth gas, $d_1 = 0.04$ m ($p_1 = 0.1$) and $d_2 = 0.36$ m ($p_2 = 0.9$)
- E5—3.5-km-depth gas, $d_1 = 0.2$ m ($p_1 = 0.5$) and $d_2 = 0.2$ m ($p_2 = 0.5$)
- E6—3.5-km-depth gas, $d_1 = 0.36$ m ($p_1 = 0.9$) and $d_2 = 0.04$ m ($p_2 = 0.1$).

Figure 5 shows that the attenuation has a maximum for a small amount of gas, approximately 10% saturation. The relaxation frequency is lower when there is more water than gas, in agreement with equation 15, where d_1 is the thickness of the water-saturated layer. Moreover, the loss is higher at shallow depths, where gas is more compliant.

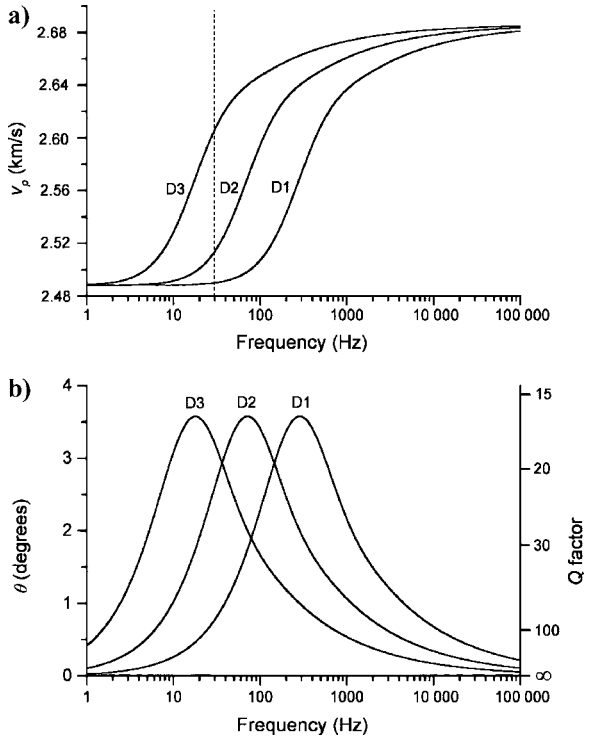

Figure 4. Phase velocity (a) and phase angle (and quality factor) (b) for a sandstone saturated with water and gas. The curves correspond to different layer thicknesses: D1: $d_1 = d_2 = 0.1$ m; D2: $d_1 = d_2 = 0.2$ m; D3: $d_1 = d_2 = 0.4$ m.

Case F

We consider two frames: sandstone, whose properties are $K_{s_1} = 37$ GPa, $\mu_{s_1} = 44$ GPa, $\rho_{s_1} = 2650$ Kg/m^3 (quartz), $\phi = 0.3$, $K_{m_1} = 4.8$ GPa, $\mu_{m_1} = 5.7$ GPa, and $\kappa_1 = 1$ Darcy, and shale, with $K_{s_2} = 25$ GPa, $\mu_{s_2} = 9$ GPa, $\rho_{s_2} = 2550$ Kg/m^3 (clay), $\phi = 0.3$, $K_{m_2} = 3.3$ GPa, $\mu_{m_2} = 1.2$ GPa, and $\kappa_2 = 1.5 \times 10^{-5}$ Darcy ($D_2 = 0.3$ μm). We assume $d_1 = 0.045$ m and $d_2 = 0.005$ m. The subcases are:

- F1—The two media are shale. Medium 1 is saturated with water, and medium 2 is saturated with gas at 1-km-depth conditions
- F2—Medium 1 is sandstone, saturated with water, and medium 2 is shale, saturated with gas at 1-km-depth conditions
- F3—Medium 1 is sandstone, saturated with gas at 1-km-depth conditions, and medium 2 is shale, saturated with water
- F4—Medium 1 is sandstone, and medium 2 is shale. Both media are saturated with water
- F5—Medium 1 is sandstone, and medium 2 is shale. Both media are saturated with gas at 1-km-depth conditions.

As shown in Figure 6, when both media are shale (curve F1) the attenuation is high at very low frequencies, and there is no relaxation peak because of the low permeability. Hence, the seismic band is at the unrelaxed state. For increasing permeability (as in case E2, where the host rock is a sandstone), the maximum attenuation occurs at seismic frequencies (exploration band). Regarding the sandstone-shale composite medium, full water saturation (F4)

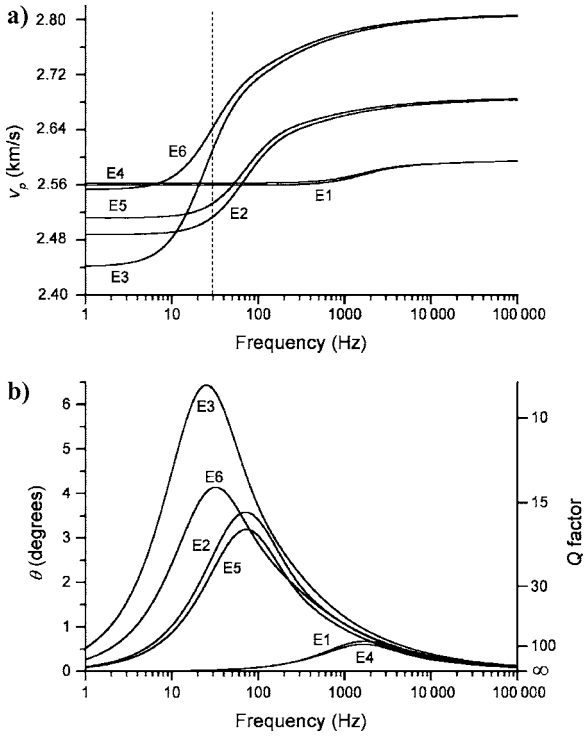

Figure 5. Phase velocity (a) and phase angle (and quality factor) (b) for a sandstone saturated with water (medium 1) and gas. The curves refer to different partial saturations, with E1, E2, and E3 corresponding to 1-km-depth gas and E4, E5, and E6 corresponding to 3.5-km-depth gas. Water saturations are: E1 and E4: 10%; E2 and E5: 50%; E3 and E6: 90%.

generates more attenuation than full gas saturation (F5), which is practically lossless. As expected, fluid-property contrasts (F2 and F3) generate significant loss and dispersion, with case F3 having a narrower peak than case F2.

Our results agree with those of other authors, who investigated some of the cases presented here. Case E3 has been analyzed by White et al. (1975) and Norris (1993), while Gurevich and Lopatnikov (1995) investigated cases E3 and F4.

Finally, it is important to note that all the results are valid only for those frequencies such that the wavelength (phase velocity divided by frequency) is large compared to the layer thickness.

DISCUSSION AND RELEVANCE FOR SEISMIC EXPLORATION

In many cases, it is difficult to distinguish between scattering effects and intrinsic attenuation. Let us consider a specific example. A typical case is when the sediments are fully or partially saturated with gas hydrates (Gei and Carcione, 2003). Bottom simulating reflectors (BSR) are interpreted to represent the seismic signature of the base of gas-hydrate formation. Below the BSR, the sediment is partially saturated with gas, and most probably with gas-pocket sizes that induce a mesoscopic-loss mechanism at seismic frequencies, because usually low frequencies are observed below the BSR. Besides the Biot and mesoscopic-loss mechanisms, scattering attenuation may occur, above and below the BSR, depending on the sizes of the gas-hydrate heterogeneities and gas patches, respectively.

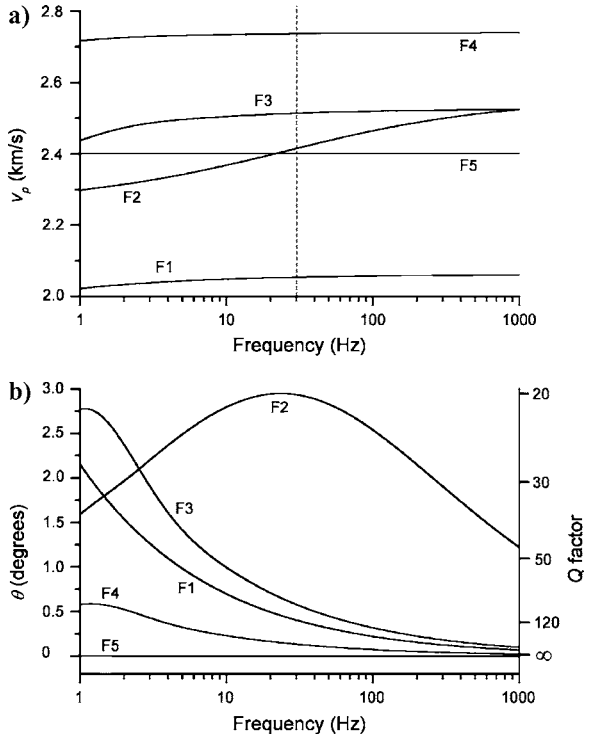

Figure 6. Phase velocity (a) and phase angle (and quality factor) (b). The curves correspond to the following cases: F1: shale (water)/shale (gas). F2: sandstone (water)/shale (gas). F3: sandstone (gas)/shale (water). F4: sandstone (water)/shale (water). F5: sandstone (gas)/shale (gas).

We have seen in the previous section (case E) that for gas patches of the order of centimeters to tens of centimeters, the mesoscopic-loss mechanism is present at seismic frequencies with realistic values of the quality factor, and this fact may explain the low frequencies below the BSR. Let us evaluate the location of the scattering relaxation peak. The corresponding relaxation frequency is

$$f_s = \frac{v_P}{2\pi h} \tag{23}$$

(e.g., Gurevich et al., 1997), where h is the average size of the heterogeneities and v_P is the average phase velocity of the P-wave. For v_P = 2.7 km/s (e.g., Carcione and Gei, 2004) and h = 10 cm, the peak frequency is 4.3 kHz. In order to have a peak at, e.g., 20 Hz, the value of h should be nearly 20 m. This is a too-high value of the patch size in the hydrate and free-gas zones. The most probable case may be that when gas hydrate is cementing the grains and, in addition, replacing the pore fluid, the attenuation is decreasing above the BSR, while the frequency loss below the BSR is solely because of the mesoscopic-loss mechanism.

The low-frequency content of seismic bright spots (Rutherford and Williams, 1989) can be because of the mesoscopic-loss mechanism, induced by partial saturation at mesoscopic scales at the gas/oil and gas/water contacts, which are not sharp interfaces, but gradual transitions. Another effect that could be explained by this mechanism is the presence of gas clouds (low signal-to-noise ratio) in offshore P-wave seismic sections (Kommedal et al., 1997). The presence of gas, leaked from the reservoir to the overburden, has the effect of both lowering seismic velocities and increasing seismic attenuation, producing low signal-to-noise ratio P-wave sections [see the numerical simulation in Carcione (1998)]. These effects are not observed in P-S sections. Then, the explanation is the presence of patchy saturation in the overburden, causing losses of mesoscopic-scale nature. The S-wave is not affected, since its energy is mainly transported through the frame of the rocks.

Finally, loss due to mesoscopic-scale heterogeneities, i.e., conversion of fast P-wave energy to slow diffusive modes, has been modeled in 1D numerical experiments performed by Turgut and Yamamoto (1988) in finely layered marine sediments.

CONCLUSIONS

Mesoscopic loss is the most probable attenuation mechanism at seismic frequencies since the amount of attenuation and velocity dispersion can be related to the microstructural characteristics of the rock and its pore fill. Information, such as permeability, porosity, fluid modulus, and viscosity, may, in principle, be inferred from the amplitude and relative propagation time of the seismic pulse.

The amount of loss because of fluid-modulus and porosity variations (spatial heterogeneities) is more important compared to other cases, such as variations of the grain and dry-rock (frame) moduli. This is the case when the contrast between the two layers of a given property is changed by the same percentage, while all other properties remain constant.

In the case of the same host rock with uniform frame properties, the maximum loss is obtained when the contrast in fluid properties is significant, for instance, in the case of a small amount of gas (around 10% saturation) in a water-saturated, highly permeable sandstone. In the case of a shale host rock, the maximum attenua-

tion is present at very low frequencies outside the seismic-exploration band, which is located at the unrelaxed state.

The relaxation peak moves towards high frequencies for increasing (background) permeability, and it is the permeability of the region hosting the stiffest fluid that determines the location of the relaxation peak (these features have been observed in a sandstone partially saturated with gas and water). Moreover, the results show that the relaxation peak moves towards low frequencies for increasing (oil) viscosity, and the maximum loss decreases (observed in a sandstone partially saturated with oil and water).

As the thickness of the layer hosting the stiffest fluid increases, the relaxation peak moves towards low frequencies. Another important feature, observed in rocks partially saturated with gas, is that the attenuation is higher at shallow depths, where gas is more compliant. Regarding sandstone-shale composite media, full water saturation generates more attenuation than full gas saturation, which is practically lossless.

In summary, measurements of the quality factor at low (seismic) frequencies may provide useful information about the fluid type and saturation, and structure of the host reservoir rock.

ACKNOWLEDGMENT

This work was financed in part by Norsk Hydro.

REFERENCES

Arntsen, B., and J. M. Carcione, 2001, Numerical simulation of the Biot slow wave in water-saturated Nivelsteiner sandstone: Geophysics, **66**, 890–896.

Ben-Menahem, A., and S. G. Singh, 1981, Seismic waves and sources: Springer-Verlag New-York Inc.

Biot, M. A., 1962, Mechanics of deformation and acoustic propagation in porous media: Journal of Applied Physics, **33**, 1482–1498.

Cadoret, T., D. Marion, and B. Zinszner, 1995, Influence of frequency and fluid distribution on elastic wave velocities in partially saturated limestones: Journal of Geophysical Research, **100**, 9789–9803.

Carcione, J. M., 1998, Viscoelastic effective rheologies for modeling wave propagation in porous media: Geophysical Prospecting, **46**, 249–270.

———, 2001, Wave fields in real media: Wave propagation in anisotropic, anelastic and porous media: Handbook of Geophysical Exploration, **31**, Pergamon Press, Inc.

Carcione, J. M., and D. Gei, 2004, Gas hydrate concentration estimated from P- and S-wave velocities at the Mallik 2L-38 research well, Mackenzie Delta, Canada: Journal of Applied Geophysics, **56**, 73–78.

Carcione, J. M., H. B. Helle, and N. H. Pham, 2003, White's model for wave propagation in partially saturated rocks: Comparison with poroelastic numerical experiments: Geophysics, **68**, 1389–1398.

Diallo, M. S., M. Prasad, and E. Appel, 2003, Comparison between experimental results and theoretical predictions for P-wave velocity and attenuation at ultrasonic frequency: Wave Motion, **37**, 1–16.

Dutta, N. C., and H. Odé, 1979a, Attenuation and dispersion of compressional waves in fluid-filled porous rocks with partial gas saturation (White model)—Part I: Biot theory: Geophysics, **44**, 1777–1788.

———, 1979b, Attenuation and dispersion of compressional waves in fluid-filled porous rocks with partial gas saturation (White model)—Part II, Results: Geophysics, **44**, 1789–1805.

Dutta, N. C., and A. J. Seriff, 1979, On White's model of attenuation in rocks with partial saturation: Geophysics, **44**, 1806–1812.

Dvorkin, J., G. Mavko, and A. Nur, 1995, Squirt flow in fully saturated rocks: Geophysics, **60**, 97–107.

Friedman, A. S., 1963, Pressure-volume-temperature relationships of gases, virial coefficients, in American Institute of Physics Handbook: McGraw-Hill Book Co.

Geertsma, J., and D. C. Smit, 1961, Some aspects of elastic wave propagation in fluid-saturated porous solids: Geophysics, **26**, 169–181.

Gei, D., and J. M. Carcione, 2003, Acoustic properties of sediments saturated with gas hydrate, free gas and water: Geophysical Prospecting, **51**, 141–157.

Gelinsky, S., and S. A. Shapiro, 1997, Dynamic-equivalent medium approach for thinly layered saturated sediments: Geophysical Journal International, **128**, F1–F4.

Gurevich, B., and S. L. Lopatnikov, 1995, Velocity and attenuation of elastic waves in finely layered porous rocks: Geophysical Journal International, **121**, 933–947.

Gurevich, B., V. B. Zyrianov, and S. L. Lopatnikov, 1997, Seismic attenuation in finely layered porous rocks: Effects of fluid flow and scattering: Geophysics, **62**, 319–324.

Helle, H. B., N. H. Pham, and J. M. Carcione, 2003, Velocity and attenuation in partially saturated rocks-Poroelastic numerical experiments: Geophysical Prospecting, **51**, 551–566.

Hill, R., 1964, Theory of mechanical properties of fiber-strengthened materials: Journal of the Mechanics and Physics of Solids, **11**, 357–372.

Johnson, D. L., 2001, Theory of frequency dependent acoustics in patchy-saturated porous media: Journal of the Acoustical Society of America, **110**, 682–694.

Jones, T. D., 1986, Pore-fluids and frequency dependent-wave propagation rocks: Geophysics, **51**, 1939–1953.

Knight, R., and R. Nolen-Hoeksema, 1990, A laboratory study of the dependence of elastic wave velocities on pore scale fluid distribution: Geophysical Research Letters, **17**, 1529–1532.

Kommedal, J. H., O. I. Barkved, and L. Thomsen, 1997, Acquisition of 4 component OBS data — A case study from the Valhall field: 59th Annual International Meeting of the European Association of Exploration Geophysicists, Expanded Abstracts, Paper B047.

Krief, M., J. Garat, J. Stellingwerff, and J. Ventre, 1990, A petrophysical interpretation using the velocities of P and S waves (full waveform sonic): The Log Analyst, **31**, 355–369.

Mavko, G., T. Mukerji, and J. Dvorkin, 1998, The rock physics handbook: Tools for seismic analysis in porous media: Cambridge University Press.

Mochizuki, S., 1982, Attenuation in partially saturated rocks: Journal of Geophysical Research, **87**, 8598–8604.

Morse, P. M., and K. U. Ingard, 1986, Theoretical acoustics: Princeton University Press.

Müller, T. M., and B. Gurevich, 2004a, One-dimensional random patchy saturation model for velocity and attenuation in porous rocks: Geophysics, **69**, 1166–1172.

———, 2004b, Seismic attenuation and dispersion due to wave-induced flow in 3-D inhomogeneous porous rocks: 74th Annual International Meeting of the Society of Exploration Geophysicists, Expanded Abstracts.

Murphy, W. F., 1982, Effects of microstructure and pore fluids on the acoustic properties of granular sedimentary materials, Ph.D. thesis, Stanford University.

Norris, A. N., 1993, Low-frequency dispersion and attenuation in partially saturated rocks: Journal of the Acoustical Society of America, **94**, 359–370.

O'Connell, R., and B. Budiansky, 1974, Seismic velocities in dry and saturated cracked solids: Journal of Geophysical Research, **79**, 5412–5426.

Pride, S. R., J. G. Berryman, and J. M. Harris, 2004, Seismic attenuation due to wave-induced flow: Journal of Geophysical Research, **109**, B01201 doi:10.1029/2003JB002639.

Rutherford, S. R., and R. H. Williams, 1989, Amplitude-versus-offset variations in gas sands: Geophysics, **54**, 680–688.

Shapiro, S. A., and T. M. Müller, 1999, Seismic signatures of permeability in heterogeneous porous media: Geophysics, **64**, 99–103.

Turgut, A., and T. Yamamoto, 1988, Synthetic seismograms for marine sediments and determination of porosity and permeability: Geophysics, **53**, 1056–1067.

White, J. E., 1975, Computed seismic speeds and attenuation in rocks with partial gas saturation: Geophysics, **40**, 224–232.

White, J. E., N. G. Mikhaylova, and F. M. Lyakhovitskiy, 1975, Low-frequency seismic waves in fluid saturated layered rocks: Izvestija Academy of Sciences USSR, Physics of the Solid Earth, **11**, 654–659.

Wood, A. W., 1955, A textbook of sound: MacMillan Publishing Company.